Geomech. Geophys. Geo-energ. Geo-resour. (2022) 8:181
https://doi.org/10.1007/s40948-022-00486-z

ORIGINAL ARTICLE

Influence of initial microcracks on the dynamic mechanical characteristics of sandstone

Shaohua Li · Kai Liu · Luke Griffiths · Chongfeng Chen · Xiaohu Yao

Received: 24 August 2021 / Accepted: 16 September 2022

Abstract Microcracks are pervasive within rock in active fault zone or geotechnical engineering and strongly influence the dynamic characteristics of rock. Here we performed dynamic compression test of sandstone to clarify the effect of initial microcracks on the mechanical performance. The different initial microcrack density levels were generated by repetitive impact loading, which was quantified using an image process method based on scanning electron microscope. Then, the strength, fragmentation, fracture propagation and energy dissipation of sandstone with different initial microcrack densities were studied using Split Hopkinson Pressure Bar apparatus. Results reveal that the strength of sandstone decreases with the increase microcrack density at a given strain rate, while, the dynamic increase factor of sandstone increases with increasing microcrack density. The sensitivity of fragmentation fractal dimension and dissipated energy to strain rate depend on the initial microcracks density. Moreover, the fractal dimension of fragmentation becomes more sensitive to the energy absorption with the increase of initial microcrack density. The present results contribute to understand the evolution of active fault and safety evaluation of geotechnical engineering.

Article highlights

- The initial microcrack density was quantified based on SEM combining with an image process method.
- The DIF of sandstone increases with increasing microcrack density.
- The fractal dimension of fragmentation becomes more sensitive to the energy absorption with the increase of initial microcrack density.

Keywords Initial microcracks · Pulverization · Microcrack density · Fractal dimension · Dissipated energy

S. Li · X. Yao (✉)
School of Civil Engineering, Wuhan University, Wuhan 430072, People's Republic of China
e-mail: yaoxh@scut.edu.cn

S. Li
Department of Engineering Mechanics, South China University of Technology, Guangzhou 510640, People's Republic of China

K. Liu (✉)
Department of Engineering Science, University of Oxford, Parks Road, Oxford OX1 3PJ, UK
e-mail: kai.liu@eng.ox.ac.uk

L. Griffiths
NGI – Norwegian Geotechnical Institute, 0806 Oslo, Norway

C. Chen
Xi'an Research Institute, China Coal Technology and Engineering Group, Xi'an 710054, People's Republic of China

Published online: 22 October 2022

1 Introduction

As a common geomaterial, rock materials, widely distributed in the earth's crust, are vulnerable to dynamic loadings, generated from earthquake, explosive volcanic activity, rock bursts or drilling and blasting (Ahsan et al. 2015; Braunagel and Griffith 2019; Doan and Gary 2009; Zhou et al. 2010), etc. Characterization of the dynamic characteristics of rock material is of great importance to understand the evolution of active fault and the stability evaluation of geotechnical engineering (Chen et al. 2020; Ma et al. 2020; Moosavi et al. 2018; Roy and Singh 2016). Many studies have investigated the mechanical performance of rock materials under dynamic loading (Cai et al. 2020; Field et al. 2004; Li et al. 2008; Zhang and Zhao 2014a, b). During dynamic loading the strain rate may range from 10^{-1} to 10^{4} s^{-1} and the strength, energy absorption and fragmentation of rock materials have been shown to related to the strain rate (Huang and Xia 2015; Li et al. 2020a, b; Wang et al. 2017; Xia and Yao 2015).

Over its lifetime, rock may undergo pervasive damage from a range of stress sources–from tectonic activity or rock blasting (Doan and d'Hour 2012; Hudson et al. 2009; Souley et al. 2001). As shown in Fig. 1, the upper custal fault zones typically contain a fracture damage zone, where rock contains different levels of initial microcracks (Aben et al. 2016). Based on the field research, these initial microcracks are supposed to influene the mechanical response to seismic activity (Andrews 2005; Faulkner et al. 2006; Griffith et al. 2012; Huang et al. 2014). Moreover, for the geotechnical egineering, it has been reported that an internal damage zone was caused by the blasting within the underground research laboratory (Martino and Chandler 2004). In mining engineering, rocks may also encounter dynamic loading such as by blasting, or impact from adjacent rock structures, leading to different levels of initial microcrack damage (Li et al. 2018a, b; Yan 2007; Zhou et al. 2010).

Many previous researches have demonstrated the strain rate sensitivity of rock is resulted from the transition of propagation and coalescence of microcracks under different loading rate (Wu et al. 2015; Zuo et al. 2006). The study of Kipp and Grady indicates that the strain-rate related fracture of rock is the result of a structural response of microcracks, the propagation and interaction of which are strain rate sensitive (Grady and Kipp 1979; Kipp et al. 1980). In addition, more pulverized granite has been observed to be localized within a few kilometers of the fault, where higher microcracks level related to successive loadings are generated in granite (Aben et al. 2016; Mitchell et al. 2011). Few researches have proven the effect of initial microcrack damage on the dynamic performance of rock materials. It is concluded that the dynamic fracture resistance of marble sample decreased with the increase cumulative damage (Yu et al. 2020). Moreover, at low strain rate, the threshold of pulverization of granite was reported to be roughly proportional to the sample strength (Doan and d'Hour 2012). These studies advanced our knowledge of the effect of initial microcracks damage on the dynamic mechanical characteristics of rock materials.

During the earthquake rupture propagation, the energy from stress wave will be dissipated by microcracks for the initiation, propagation and interaction, resulting in deformation and failure of rock materials (Andrews 2005; Chen et al. 2009; Zhang and Zhao 2014a, b). Given that the initial microcracks have been proven to influence the fracture and threshold of pulverization of rock, it can be expected that the microcracks would influence the strength, energy absorption and fragmentation characteristics of rock under dynamic loading. However, the effect of initial microcracks on the strength and relationship between the energy absorption and fragmentation of rock, which is of vital importance to understand the temporal and spatial evolution of active fault and safety evaluation of geotechnical engineering, has not been reported.

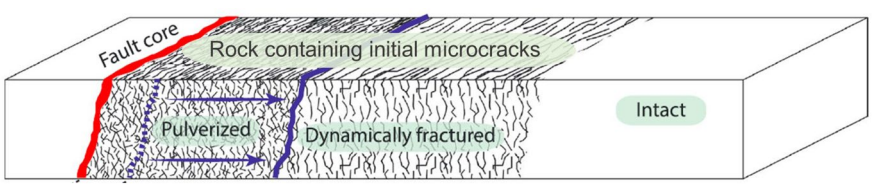

Fig. 1 Schematic of fault zone consisted by rock containing initial microcracks (Aben et al. 2016)

To this aim, we applied repetitive impact loading on sandstone to create varying degrees of microcracks damage, which we quantified through analysis of SEM micrographs combining an image process method. Then, split Hopkinson pressure bar (SHPB) device was used to test the dynamic performance of sandstone with different microcrack densities. We explored the effect of the initial microcracks on the strength and relationship between the energy absorption and fragmentation of sandstone under dynamic loading and clarify the corresponding mechanism. The results obtained from this study would help with elucidating the evolution of active fault and design and stability evaluation of geotechnical engineering made of rock materials.

2 Materials and experimental methods

2.1 Rock material and preparation

To make sure the comparison in this study, the sandstone samples for experiment were cored from a single block from a quarry, China. The physical and mechanical parameters of the samples are shown in Table 1. The diameter and length of the cylindrical sandstone sample used for compression tests were both 50 mm, to eliminate radial and axial inertial effects (Zhang and Zhao 2014a, b). A strict tolerance of ± 0.02 mm was selected as the precision of the samples ends. The compressive strength under uniaxial loading of the sandstone is 45.9 MPa. The stress–strain curve at the quasi-static uniaxial compression is shown in Fig. 2.

Table 1 The physical and mechanical parameters of the sandstone sample

Parameter	Value
Modal composition	64% quartz, 18% feldspar, 13 cement and 5% mica
Grain size (mm)	0.2–0.5
Uniaxial compressive strength (MPa)	45.9
Tensile strength (MPa)	3.24
Elasticity modulus (GPa)	9.4
Poisson's ratio	0.29
Cohesion (MPa)	6.52
Internal friction angle (°)	29.39
Density (g/cm^3)	2.47
Porosity	4.2
P-wave velocity (m/s)	2810

2.2 Experimental methods

2.2.1 Split Hopkinson pressure bar (SHPB) apparatus

Dynamic compression experiments were carried out on SHPB device with a diameter of 74 mm in this work, shown in Fig. 3. To avoid premature failure of specimens before reaching a state of stress equilibrium, annealed copper disks were used as pulse shaper. To record the surface crack propagation behavior, a high-speed digital camera (i-SPEED 726) is used to capture image of sandstone sample during the impact process. 10 μs is set as the inter-frame time, which benefits to capture enough images before the failure of sandstone sample.

The typical three waves acquired in SHPB test are shown in Fig. 4. The stress wave is measured based on the one-dimensional wave theory, moreover, the dissipated energy is calculated based on the energy conservation assumption. More information concerning SHPB test can be found in our previous study (Li et al. 2018a, b).

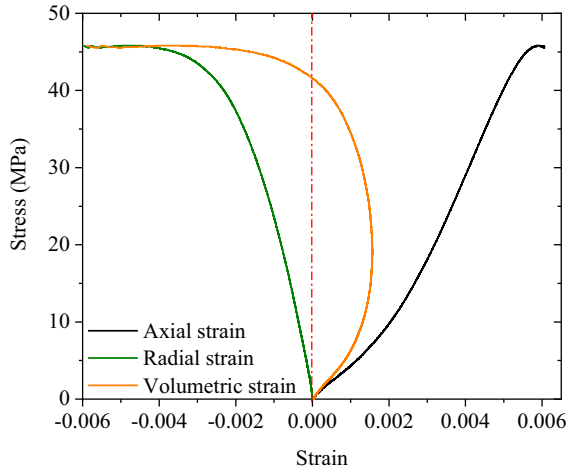

Fig. 2 Uniaxial compressive stress–strain relationship of sample

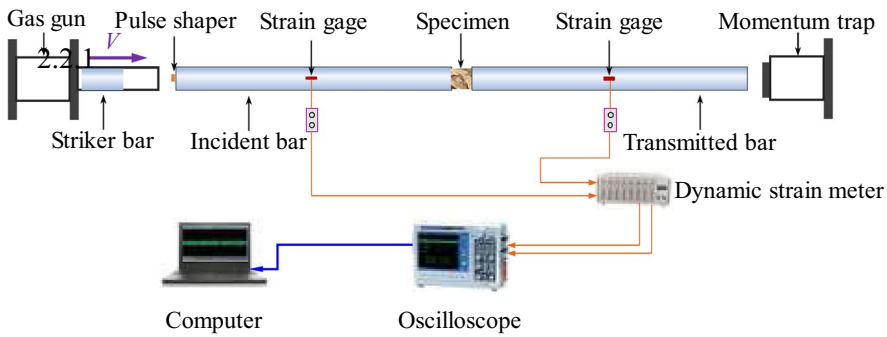

Fig. 3 The Split Hopkinson Pressure Bar (SHPB) system

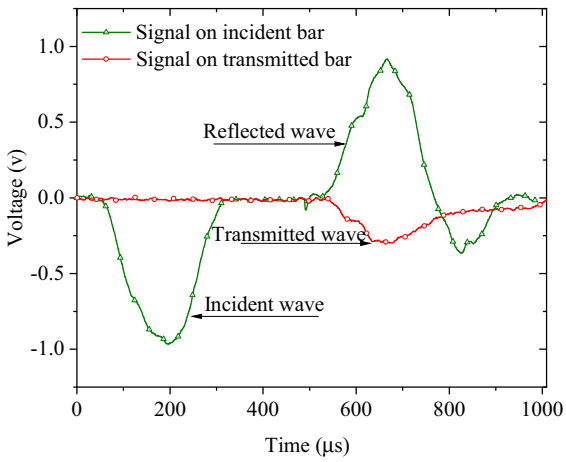

Fig. 4 Typical original wave signals captured in SHPB test

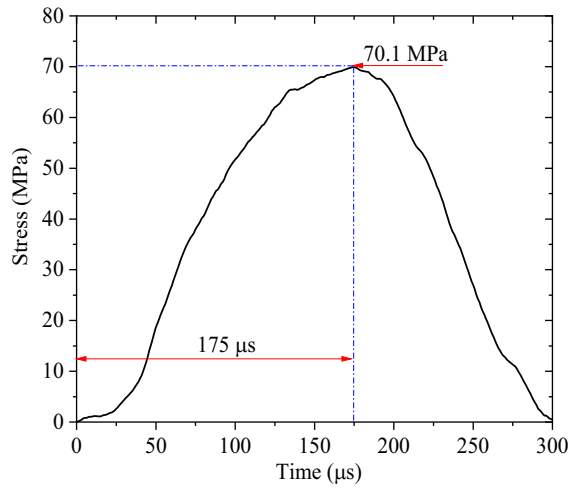

Fig. 5 Incident wave for repetitive impact loading

2.2.2 *Procedure for repetitive impact loading*

For the repetitive loading experiment, an incident stress wave was selected so that a sufficient number of impacts could be completed before failure, guaranteeing that rock samples contain different amounts of cumulated microcrack damage. For the repetitive impact experiment, an incident stress under impact velocity of 2.5 m/s, shown in Fig. 5. To achieve the stress uniformity (Xia and Yao 2015), the rising time was aet as 175 μs. The sandstone sample failed after exposition to 8 impact loadings with the same incident stress wave. Total 15 samples were used for the determination of test set for the repetitive impact loading.

2.2.3 *Procedure for single impact loading*

To investigate the dynamic performance of sandstone containing initial microcrack damage, single impact experiments were carried out on sandstone samples that had previously been exposed to different numbers (0, 4 and 6) of repetitive impact loadings. In each set of single impact loading test with the same strain, at least 5 sample were tested. Generally, the strain rate is selected as the standard for comparison (Xia and Yao 2015; Zhou et al. 2011). Due to that different initial damage would result in different elastic modulus, leading to different strain rate of sandstone exposed to same incident wave. Thus, to ensure that the sandstone specimens deformed at similar strain rates, incident waves with different loading rates were selected to impact sandstone specimens with different initial microcrack damage. The incident waves

with different loading rates were reached by adjusting the air pressure. 0.25 MPa was set as the initial level, with an increasing step of 0.025 MPa.

2.2.4 *Quantification of microcracks*

Thin sections of the sandstone samples were prepared in a plane parallel to the sandstone sample axis. Before testing, all the samples were coated with gold sputtering to enhance the electrical conductivity. Micrographs were recorded by using a scanning electron microscope (Quanta 250 FEG, Thermo Fisher scientific, USA) configured for Backscattered-Electron (BSE) imaging at an accelerating voltage of 10 kV. All the images (1024 × 1024 pixels or 1.1 mm × 1.1 mm) were at 235× magnification and taken across an area of 5.5 mm × 5.5 mm across each of the thin sections, as shown in Fig. 6. At least five regions with area of 5.5 mm × 5.5 mm were selected arbitrarily in each sample to minimize the influence of the heterogeneity of microcracks quantification.

An image process method capable of segmentation and skeletonization of microcracks was used to process the micrographs and provide the microcrack length and 2D crack density. As shown in Fig. 7, the procedure of quantification of the microcracks includes filtering, segmentation, skeletonization and calculation of microcrack length. This image process is written in Python and more detailed information can be in (Griffiths et al. 2017).

Here we use the 2D crack density, noted γ, to quantify the initial microcrack damage within the sandstone samples exposed to different repetitive loadings. The 2D crack density is defined as following (Walsh 1965):

$$\gamma = N_A c^2 \tag{1}$$

where N_A is the cracks number in unit area, c is the mean microcrack length.

3 Experimental results

3.1 Quantification of initial microcracks

The damage accumulation of rock materials have been proven to be resulted from the initiation, propagation and interaction of microcracks (Eberhardt et al. 1999). To assess the influence of repetitive impacts

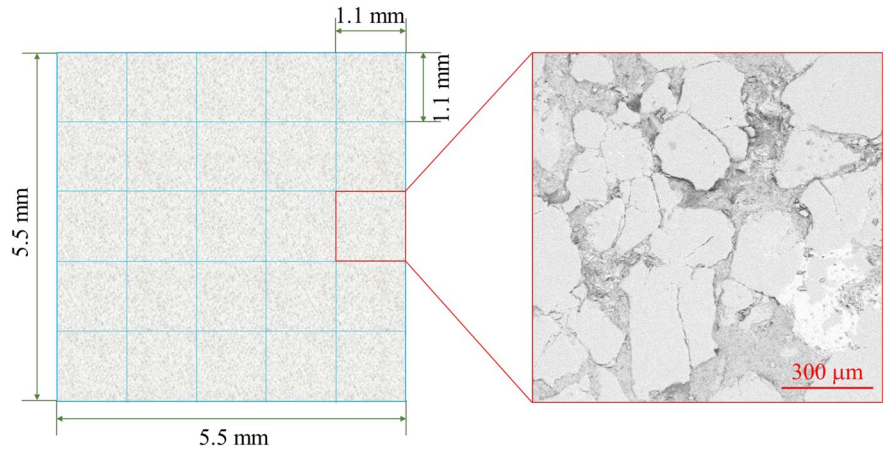

Fig. 6 BSE imaging of thin sections of sandstone samples

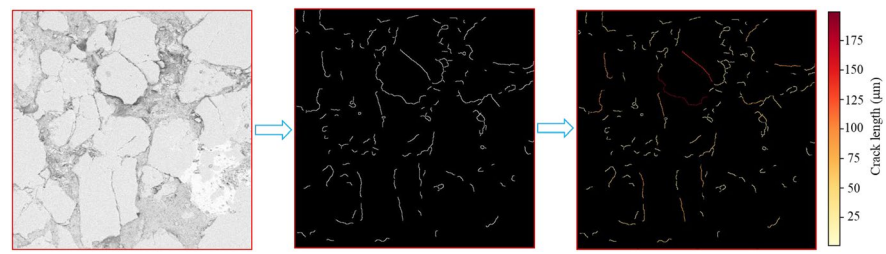

Fig. 7 Procedure of quantitatively characterize the microcracks

on the evolution of microcrack damage, we selected the samples exposed to 0, 4 and 6 impacts. As shown in Fig. 8a, for the sample with 0 impact, microcracks are mostly intergranular, following grain boundaries, and appear near-randomly distributed. The observed initial microcrack damage within the sample with 0 impact can be attributed to a range of factors, including geological history and material properties (Dresen and Guéguen 2004), as well as tectonic or blasting activity (Doan and d'Hour 2012; Hudson et al. 2009;

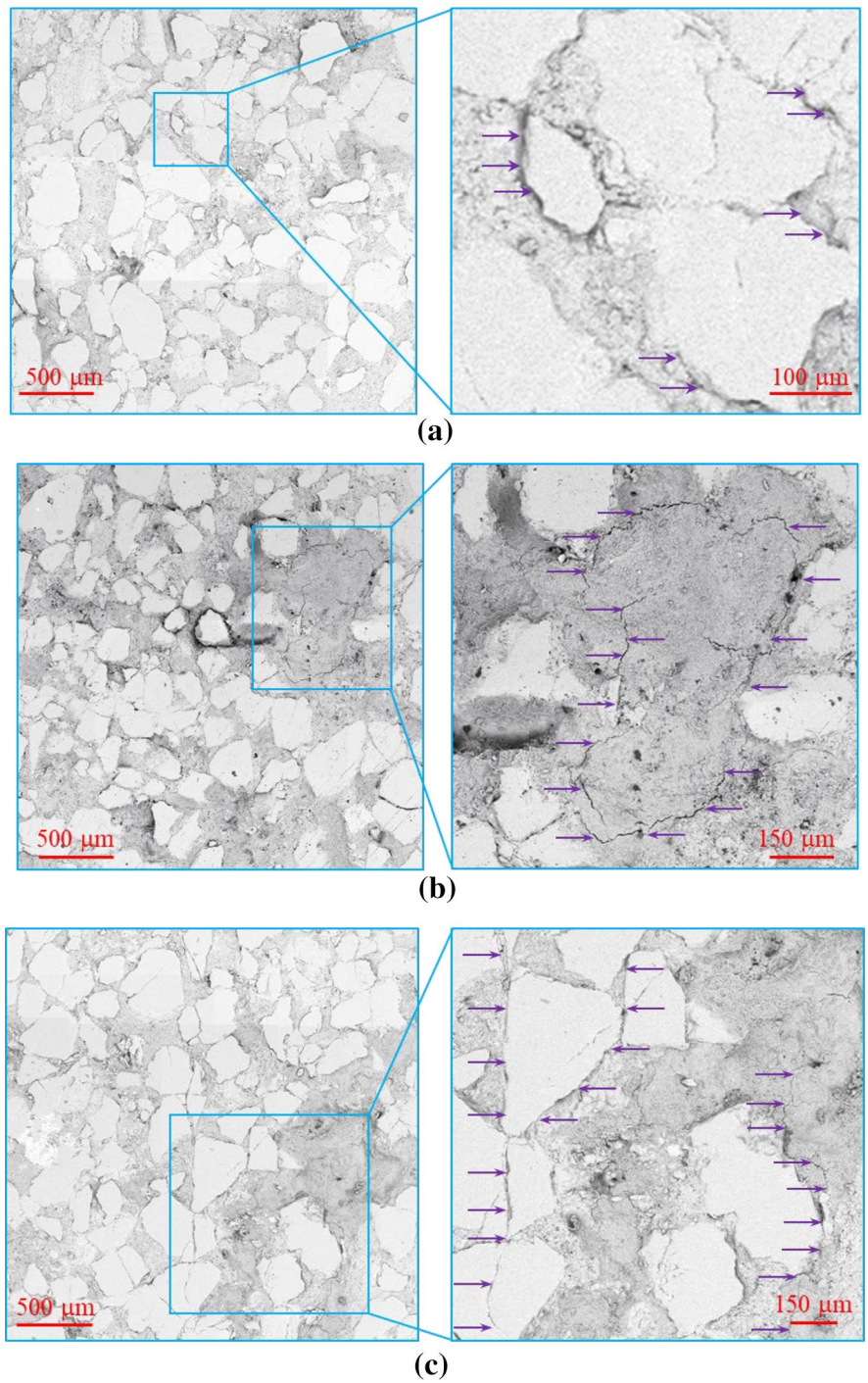

Fig. 8 The microcracks within a sandstone sample exposed to repetitive impact loading. SEM micrographs of: **a** sample exposed to 0 impacts; **b** sample exposed to 4 impacts; and **c** sample exposed to 6 impacts

Souley et al. 2001). Once the sample was exposed to 4 repetitive impacts, the length and number of microcracks show an increase tendency. Meanwhile, as shown in Fig. 8b, few long microcracks can be found around a mineral crystal, indicating that microcracks resulted from dynamic impact start to interact with each other. As shown in Fig. 8c, within the sample exposed to 6 repeated impacts, the length of microcracks increases further. We observe more microcracks along grain boundaries, and some longer microcracks spanning several grains, oriented near-parallel to the loading direction.

To quantify the microcracks damage of samples, the 2D microcrack density was analyzed. The corresponding values of N_A and c of three different crack densities are presented in Table 2. As shown in Fig. 9, some initial microcracks distribute in the sample without impact, resulting in a 2D microcrack density of 0.026. It is lower than that of Garibaldi Grey Granite, in which the initial 2D microcrack density is 0.062 (Griffiths et al. 2017). This might be attributed to different diagenetic process or loading history (Anders et al. 2014). The 2D microcrack density increases to 0.043 and 0.053 as the repetitive impact number increases to 4 and 6.

3.2 Influence of initial microcracks on the deformation and strength of sandstone

3.2.1 Quasi-static strength

The quasi-static strength of sample containing different initial microcracks is presented in Fig. 10. The quasi-static strength decreases from 45.7 to 42.3 MPa and 37.8 MPa as the initial microcrack density increases from 0.026 to 0.043 and 0.053, respectively. Undoubtedly, the quasi-static strength is sensitive to the initial microcracks, that is, a higher microcrack density level results in a lower quasi-static strength

Table 2 The microcracks information in the sample with different repetitive impact number

Repetitive impact number	N_A (mm^{-2})	c (μm)	γ
0	49.1	23	0.026
4	58.9	27	0.043
6	63.0	29	0.053

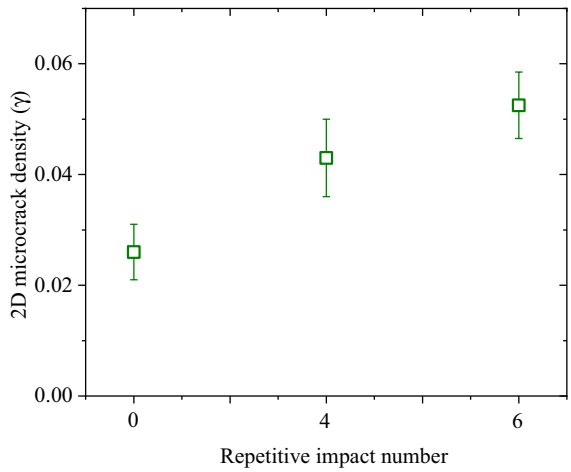

Fig. 9 2D microcrack density of sandstone sample

value. This is in line with previous results (Griffiths et al. 2017; Peng et al. 2016). This can be attributed to that a higher initial microcrack density is along with a higher crack number and a longer crack length, which leads these cracks easier to propagate and interact with each other (Ashby and Hallam 1986; Ashby and Sammis 1990).

3.2.2 Strain rate

Generally, the strain rate is selected as the reference for evaluating the deformation characteristics of rock

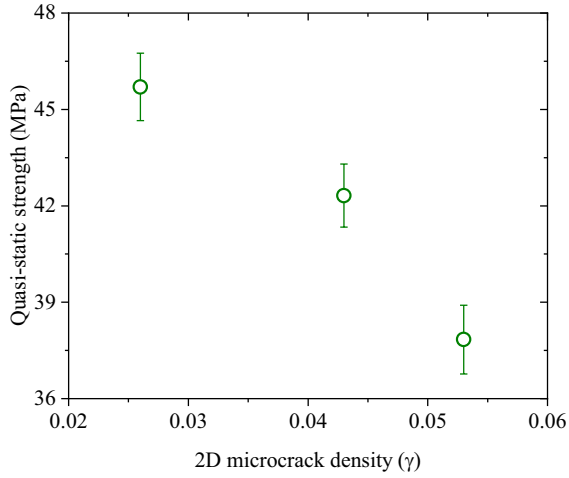

Fig. 10 Quasi-static strength of sample containing different initial microcracks

materials (Xia and Yao 2015; Zhou et al. 2011). Here, to compare tests on sandstone samples with different initial microcrack damage, the influence of gas pressure on the strain rate of sample with various microcrack densities was analyzed. The minimum gas pressure was 0.25 MPa, the maximum was 0.55 MPa, and the step between measurements was 0.025 MPa. As shown in Fig. 11, the strain rate of sandstone sample increases with increasing gas pressure in a quasi-linear way. For a given air pressure, the strain rate is higher for samples with a higher microcrack damage level, which is similar to previous results from repetitive loading experiments (Li et al. 2018a, b). As the strain rate is calculated based on the reflected stress wave, the increase in strain rate for a given gas pressure indicates a decrease in impedance of the sandstone sample. The decrease in impedance is resulted from the degradation of sandstone sample exposed to different impact loadings (Li et al. 2005; Zhou et al. 2018).

3.2.3 *Stress–strain relationship*

To clarify the effect of initial microcracks on the dynamic performance of the sandstone sample, the stress–strain response of sandstone with different repetitive impact loadings under similar strain rate (~80 s^{-1}) were analyzed. As shown in Fig. 12, at the similar strain rate (~80 s^{-1}), the stress–strain response of sandstone samples containing different initial microcrack densities show some obvious differences. Within the initial linear elastic section of the stress–strain curve, the slope of the curve decreases with increasing initial damage. The decrease in the slope of the curve could be attributed to the degradation of elastic modulus of sandstone sample due to the impact damage. However, given that the dynamic stress uniformity can't be reached during the most part of the elastic loading stage, the specific elastic modulus value can't be calculated based on the stress–strain curve presented in Fig. 12. We measure a decrease in peak stress with increasing initial microcrack density, while strain at the peak stress increases with the increase initial microcracks. For the sample with microcrack density of 0.053, the post-peak stress–strain behavior differs to the other two samples, showing an increase in strain as the stress drops. The increase in strain may be related to the different failure pattern of sandstone sample with different initial damage. Deformed at a strain rate of 100 s^{-1}, the sample with microcrack density of 0.053 was pulverized, whilst the samples exposed to 0 and 4 repetitive impacts were still of some bearing capacity. It can be deduced that the threshold of pulverization of sandstone sample exposed to 6 repetitive impact is no higher than 80 s^{-1}, while the thresholds of pulverization of samples with initial microcrack densities of 0.026 and 0.043 are higher than 80 s^{-1}. This means that the initial microcrack damage would lead to the change of failure pattern of sandstone sample at the

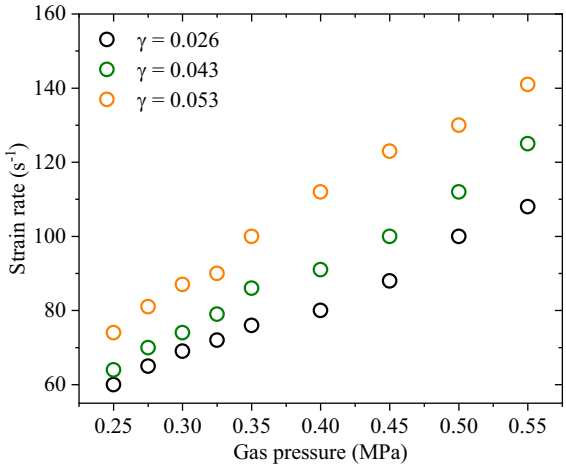

Fig. 11 Strain rate of samples containing different initial microcracks

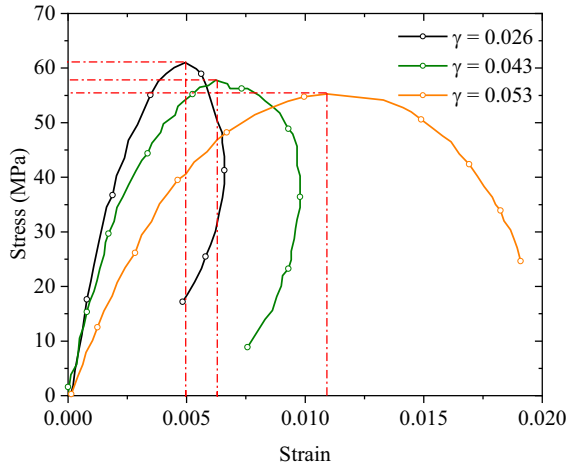

Fig. 12 Stress–strain curves of samples containing different initial microcrack densities deformed at a strain rate of 80 s^{-1}

same strain rate, which is consistent with the results of (Doan and d'Hour 2012; Doan and Gary 2009).

To clarify the effect of strain rate on the deformation behavior of sample with initial microcracks, here we select the sandstone sample with initial microcrack density of 0.043 for analysis. As shown in Fig. 13, the slope of the linear elastic parts of each stress–strain curve are similar for each sample, indicating that the slope of stress–strain of sandstone sample with initial microcrack damage is insensitive to the strain rate, as is the case for the rock without repetitive impact. Both the peak stress and strain value at the peak stress increase with the increase of strain rate, which is consistent with previous results of rock materials without repetitive impact (Frew et al. 2001; Li et al. 2017). Meanwhile, the secondary unloading can be found in the post-peak part of stress–strain of 79 s^{-1}, while the post-peak parts of stress–strain of 100 s^{-1} and 125 s^{-1} are just of one unloading stage. It can be deduced that the threshold of pulverization of sandstone sample is between 79 and 100 s^{-1}.

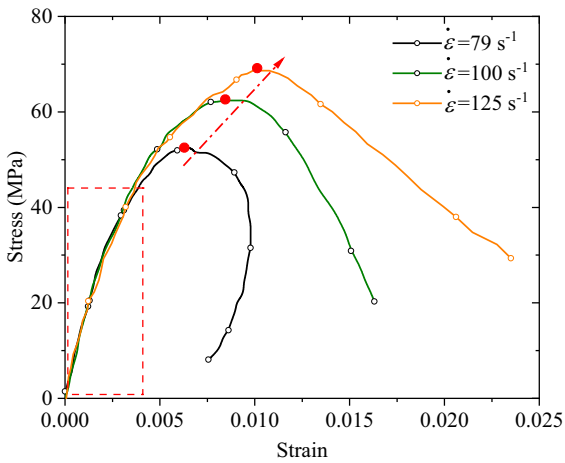

Fig. 13 Stress–strain curves for the sample with microcrack density of 0.043 deformed at strain rates of 79, 100 and 125 s^{-1}

3.2.4 *Dynamic compressive strength*

Here we analyze the rate dependence of strength of the sandstone containing initial microcrack damage. As presented in Fig. 14a, the strength of sandstone is dependent to the strain rate. For a given microcrack density, the strength increases with increasing strain rate. The strength of sample without impact damage is higher than both samples exposed to repetitive impact. Figure 14b shows the DIF with strain rate, to clarify the influence of initial microcrack density on the strain rate sensitivity. As shown in Fig. 14b, for a given strain rate, the DIF increases with increasing initial microcrack density. Previous research has attributed the strain rate effect of rock materials to

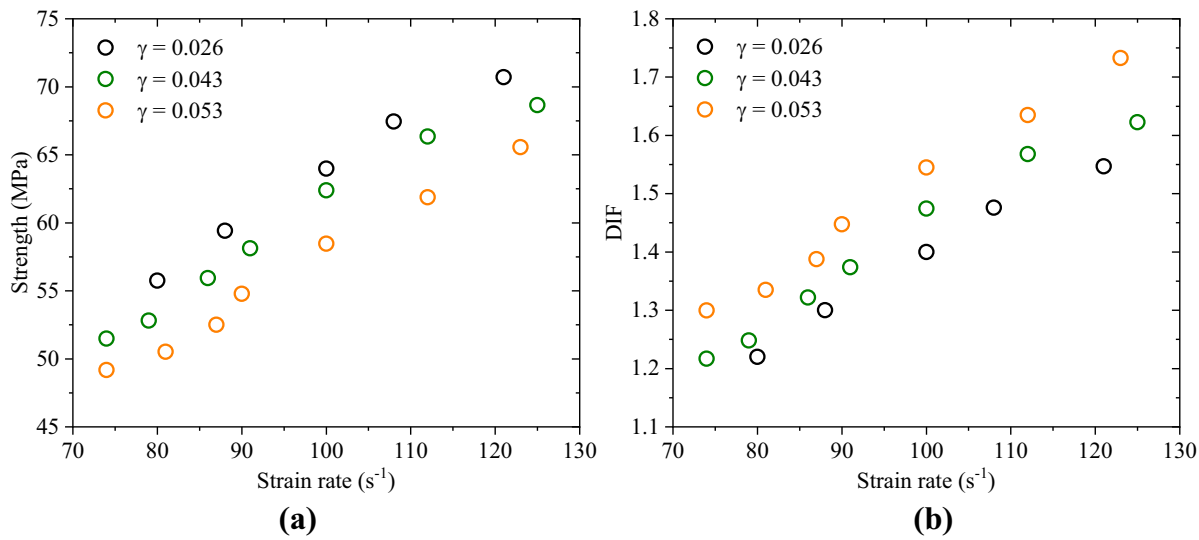

Fig. 14 Strength and dynamic increase factor (DIF) of sandstone with different initial microcrack densities. **a** Dynamic strength; **b** DIF

the heterogeneity of microstructure of rock materials (Zhu et al. 2012). Undoubtedly, with the increase of initial microcrack density, the microcracks number show a positive relationship, leading to a higher heterogeneity of microstructure of sandstone sample.

3.3 Fragmentation and energy absorption characteristics

3.3.1 Fragmentation

To elucidate the fragmentation behavior of sandstone containing different initial microcrack damages, the fragmentations of the failed sandstone samples were collected. Figure 15 shows photographs of the fragmented pieces of sandstone samples containing different initial microcrack densities, deformed at strain rates of around 80 s^{-1} and 100 s^{-1}. We observe that fragmentation characteristics of sandstone sample is strongly influenced by the strain rate, as has widely been reported in previous research (Cai et al. 2007; Yuan et al. 2011). The fragmented samples change from large split pieces to pulverized debris as the strain rate increases from 80 to 100 s^{-1}.

The mean fragmentation size of the sandstone samples with repetitive impact (initial microcrack densities of 0.043 and 0.053), reduced compared to the sample without repetitive impact damage (initial microcrack density of 0.026). This indicates that the fragmentation of sandstone sample is not just influenced by the strain rate, but also by the microcracks damage, which is consistent with the result of (Doan and d'Hour 2012). The failure of rock materials under dynamic loading has been attributed to the propagation of microcracks (Zhang and Zhao 2014a, b). The introduction of additional microcracks generated from dynamic loading would lead to more microcracks propagation simultaneously under the same strain rate, resulting in a higher degree of fragmentation, as confirmed by the result of the threshold of pulverization (Fig. 15).

Previous research has proven that rock fragmentation has self-similarity and can be quantified based on fractal dimension (Grady 2008; Grady and Winfree 2001). To quantitatively characterize the effect of initial microcrack on the pulverization characteristics of sample, the fractal dimension of sandstone sample is analyzed. The fractal dimension of rock fragmentation can be determined as follows (Xie et al. 2003):

$$Y = \frac{M(x)}{\mathrm{M_T}} = \left(\frac{x_i}{x_m}\right)^{3-D} \tag{2}$$

where $\mathrm{M_T}$ is total mass of rock fragmentation, $M(x)$ is cumulative mass of rock fragmentation with size below x_i, x_m is the maximum fragmentation size, and D is the fractal dimension of rock fragmentation.

The fractal dimension of sample under dynamic loading is shown in Fig. 16. Noting that the unbroken

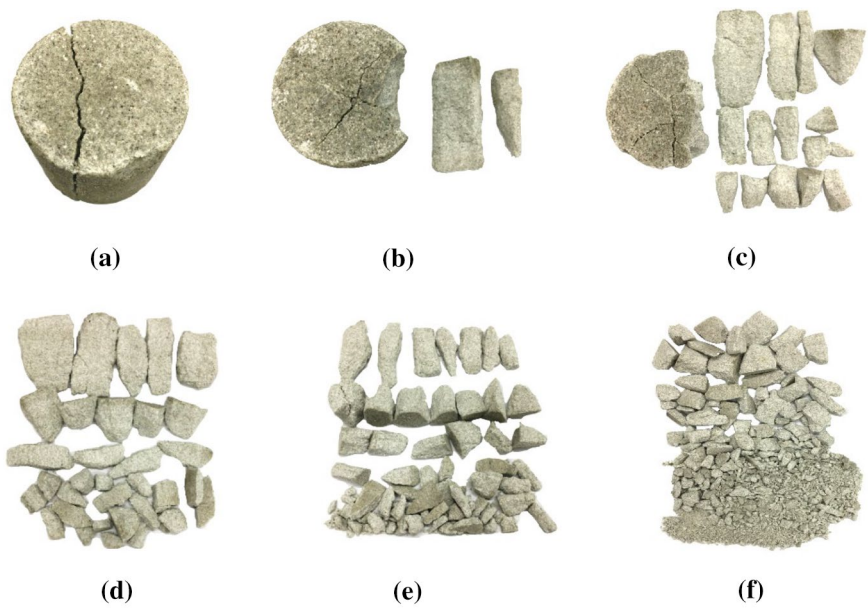

Fig. 15 Fragmentation of sandstone samples with different initial microcrack densities. **a** 80 s^{-1}; **b** 79 s^{-1}; **c** 81 s^{-1}; **d** 97 s^{-1}; **e** 100 s^{-1}; **f** 99 s^{-1}

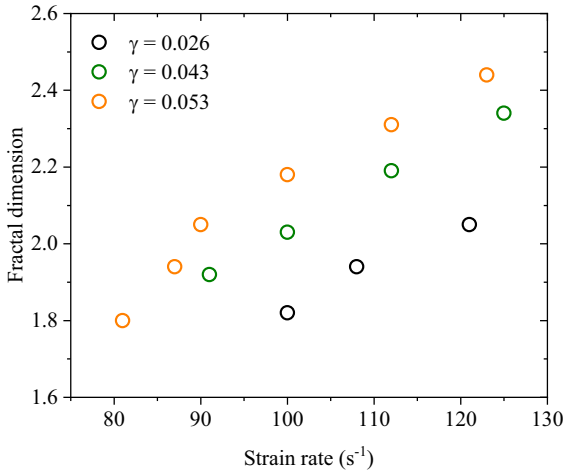

Fig. 16 Fractal dimension of the rock fragment size distribution (fragments shown in Fig. 15) against strain rate during dynamic loading. The results are shown for the sandstone samples with initial microcrack densities of 0.026, 0.043 and 0.053

and slightly split sample are excluded. Specifically, the results of sample containing microcrack densities of 0.026 under strain rate less than 100 s^{-1}, sample with microcrack densities of 0.043 under strain rate less than 90 s^{-1} and sample with microcrack densities of 0.053 under strain rate less 80 s^{-1} are excluded during the analysis processing. The fractal dimension of sandstone sample increases with the increase of strain rate, which is assigned to the decreasing size of failed sample under a higher loading rate. Meanwhile, under the same strain rate, the fractal dimension of sandstone sample increases with increasing initial microcrack density. It means that, under the same strain rate, more debris with smaller fragment size are generated during the pulverization process of sandstone sample with more microcracks. It can be deduced that higher number of microcrack propagate during the failure process of sandstone sample with more microcracks.

3.3.2 Dynamic fracture process

To give a further interpretation of the fragmentation behavior of sandstone, the surface crack propagation of sandstone is analyzed based on the high-speed camera image. The propagation of the macro-cracks under a similar strain rate, around 80 s^{-1}, are presented to clarify the effect of microcracks on the cracking process. As shown in Fig. 17, at the loading time of 100 μs, no obvious macro-crack can be observed on the surface of sandstone sample with initial microcrack density of 0.026, while few macrocracks have generated on the surface of samples with initial microcrack density of 0.043 and 0.053. With the increase of loading time, more macro-cracks are presented on the surface of sandstone samples. Meanwhile, some distinct differences can be found between samples containing different microcracks. Specifically, at the loading time of 100 μs, more macrocracks are generated on the surface of sandstone sample with initial microcrack density of 0.053, but, only about three macrocracks can be found on the surface of sample with initial microcrack density of 0.026. In addition, the length of the cracks on the surface of sample with initial microcrack density of 0.053 are longer than that of samples with fewer microcracks.

Hence, it can be concluded that the initial microcracks affect the fracture process of sandstone, leading to different fragmentation characteristics. Specifically, under the same strain rate, more microcrack will propagate simultaneously in the sandstone sample with a higher microcrack density. Based on the micromechanical theory, the microcrack start to propagate as the fracture toughness is satisfied (Li et al.

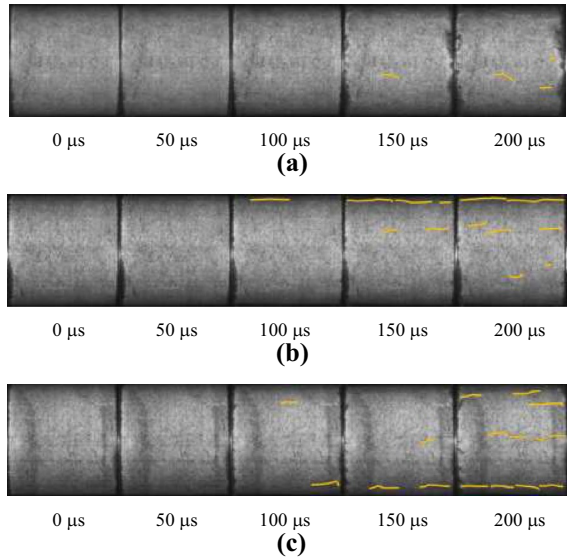

Fig. 17 Macro-cracks on the surface of sandstone during dynamic loading process. **a** sample with microcrack density of 0.026; **b** sample with microcrack density of 0.043; **c** sample with microcrack density of 0.053

2020a, b). Given that a higher microcrack density means higher values of number and length of microcracks in sandstone sample, it is expected that the microcracks are easier to propagate under the same loading conditions (Li et al. 2020a, b). It can be also responsible to the lower threshold of pulverization of sandstone with a higher microcrack density.

3.3.3 Dynamic energy dissipation

The energy absorption per unit volume under different strain rates are presented to investigate the effect of microcracks on the energy absorption capability of sandstone. As presented in Fig. 18, despite of the different initial microcrack densities, the energy absorption increases with the increase of strain rate, which is in line with other studies (Li et al. 2019, 2005). Nevertheless, the sensitivity of energy absorption capability to strain rate varies with the initial microcracks density. In the case of a lower strain rate (less than 100 s^{-1}), the energy absorption presents a positive relationship with the microcracks, while at a higher strain rate (larger than 120 s^{-1}), the energy absorption per unit volume shows a negative relationship with the microcracks. That is, there is a transition zone, where the energy absorption per unit volume is insensitive to the initial microcracks. This transition zone might be attributed to different failure patterns of sandstone samples due to different initial microcracks densities. It should keep in mind that the sandstone sample with lower microcracks density can't fail under lower strain rate (less than 80 s^{-1}), thus, less energy will be dissipated during the impact process. In contrast, the sandstone sample with higher microcracks density can fails with few pulverized debris, which will dissipate more energy for the initiation and propagation of cracks. As the strain rate increases to a higher level, all the sandstone samples will pulverize, leading to a higher energy absorption capability of sample with less microcracks than that of sandstone sample with more microcracks.

3.3.4 Relationship between fragmentation and energy absorption

The dissipated energy is used for the propagation of cracks during the impact process of sample, resulting in different fragmentation characteristics (Andrews 2005; Kipp et al. 1980). Here, to quantitatively analyze the effect of the microcrack density on the relationship between energy absorption and fragmentation of sandstone, the relationship between the energy absorption per unit volume and fractal dimension is presented.

As shown in Fig. 19, at any initial microcrack density, the fractal dimension increases with increasing energy absorption per unit volume, indicating that a more pulverized failure pattern corresponds to a higher energy absorption of sandstone. This is consistent with the previous study (Cai et al. 2020),

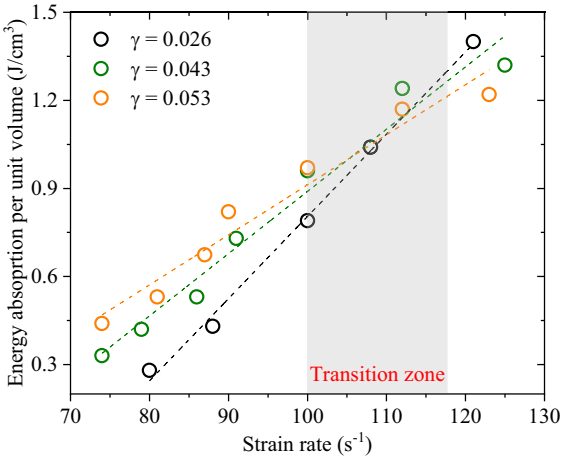

Fig. 18 Energy dissipation of sandstone containing different microcracks

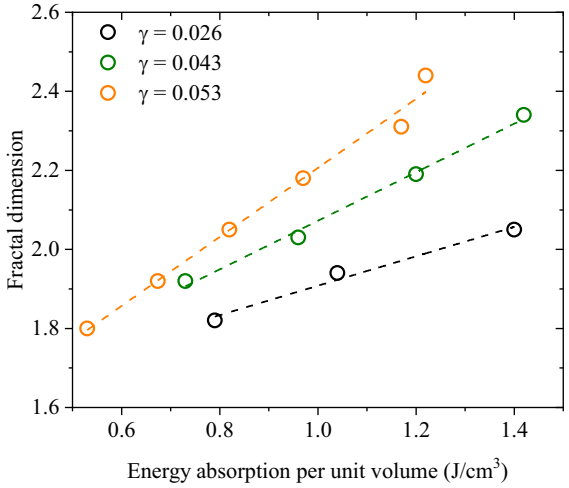

Fig. 19 Relationship between Fractal dimension and energy absorption of sandstone

which can be explained by that more cracks are activated under a higher strain rate, consuming more energy per unit volume during the impact process. Meanwhile, based on the fitting lines, the sensitivity of fractal dimension to energy absorption varies with the initial microcrack density. In the case of a higher microcracks density, the fractal dimension becomes more sensitive to the energy absorption. This could be related to the crack propagation characteristic of sample with different microcracks.

4 Implications to geoengineering

Initial Microcracks are pervasive in upper crustal fault zone, which is typically consisted with a fault core and a surrounding damage zone. The transition of the properties of rock in fault zone has been confirmed to affect the evolution of faulting as exposed to seismic cycle (Faulkner et al. 2006; Griffith et al. 2012). In addition, pulverized rocks near the fault core are found to be related to low strain rate successive seismic events (Doan and d'Hour 2012). This is inconsistent with the laboratory study concerning single impact loading experiment, which suggests that pulverization of rocks just takes place when the strain rate is higher than a certain threshold (Doan and Gary 2009; Xia et al. 2008). However, the initial microcracks would affect the fracture process of sandstone, resulting in that more microcrack will propagate simultaneously in the sandstone sample with a higher microcrack density. Hence, the strain rate threshold of pulverization decreases with the increase of initial microcrack density, suggesting that successive seismic would results in more pulverized rock along fault core. Meanwhile, during the earthquake rupture propagation, the energy dissipation of stress wave is used to further weaken the fault damage zone (Andrews 2005). Based on the experimental results, as an earthquake stress wave with lower strain rate propagates across the damage zone, the energy dissipation of sandstone increases with the increase of initial microcrack density, in contrast, as an earthquake stress wave with higher strain rate propagates across the damage zone, the energy dissipation of sandstone decreases with the increase of initial microcrack density. It is suggested that the influence of initial microcrack damage and strain rate should be considered simultaneously when analyzing the energy dissipation of earthquake rupture.

5 Conclusions

To elucidate the effect of microcrack damage on the dynamic performance of rock material, we performed compression tests at a range of strain rates on sandstone samples which had first been subjected to different numbers of repetitive impacts. Microcrack damage within the sandstone samples was quantified by calculating the microcrack density from processed SEM micrographs of thin sections. Finally, the strength, deformation, energy dissipation and degree of fragmentation of the tested samples were discussed. The following conclusions can be drawn:

- Repetitive impact leads to higher level of the number and length of microcracks within sandstone. The 2D microcrack density increases from 0.026 for the sample without repetitive impact, to 0.043 and 0.053 of samples subjected to 4 and 6 repetitive impacts.
- The strength of sandstone decreases with increasing initial microcrack density, while, the dynamic increase factor (DIF) of sandstone increases with the increase of microcrack density.
- The pulverization threshold of sandstone decreases with the increase of initial microcrack density. For a given strain rate, in the case of a higher microcracks density, more cracks propagate simultaneously resulting in a larger fractal dimension of fragmentation.
- The sensitivity of energy absorption capability of sandstone to strain rate depends on the initial microcrack density. There is a transition zone, from 100 to 120 s^{-1}, beyond which the energy absorption capability of sandstone sample shows a higher level with the increase of strain rate.
- The fractal dimension of failed sample exhibits a linear relationship with the energy absorption per unit volume. With the increase of initial microcrack density, the fractal dimension becomes more sensitive to the dissipated energy, which suggests that in the case of a higher microcracks density, more small fragments generate with the increase of dissipated energy.

Acknowledgements This research was carried out under the funding of the National Natural Science Foundation of China (Grant No. 11672110) and the National Science Fund for Distinguished Young Scholars (No. 11925203). This work also benefits from the Fundamental Research Funds for the Central Universities, SCUT (2018PY21).

Declarations

Conflict of interest The authors declare that they have no conflict of interest regarding the publication of this paper.

References

Aben FM, Doan M, Mitchell TM, Toussaint R, Reuschlé T, Fondriest M, Gratier J, Renard F (2016) Dynamic fracturing by successive coseismic loadings leads to pulverization in active fault zones. J Geophys Res Solid Earth 121:2338–2360

Ahsan N, Scheding S, Monteiro ST, Leung R, McHugh C, Robinson D (2015) Adaptive sampling applied to blasthole drilling in surface mining. Int J Rock Mech Min Sci 75:244–255

Anders MH, Laubach SE, Scholz CH (2014) Microfractures: a review. J Struct Geol 69:377–394

Andrews DJ (2005) Rupture dynamics with energy loss outside the slip zone. J Geophys Res Solid Earth 110

Ashby MF, Hallam SD (1986) The failure of brittle solids containing small cracks under compressive stress states. Acta Metall 34:497–510

Ashby MF, Sammis CG (1990) The damage mechanics of brittle solids in compression. Pure Appl Geophys 133:489–521

Braunagel MJ, Griffith WA (2019) The effect of dynamic stress cycling on the compressive strength of rocks. Geophys Res Lett 46:6479–6486

Cai M, Kaiser PK, Suorineni F, Su K (2007) A study on the dynamic behavior of the Meuse/Haute-Marne argillite. Phys Chem Earth Parts a/b/c 32:907–916

Cai X, Zhou Z, Zang H, Song Z (2020) Water saturation effects on dynamic behavior and microstructure damage of sandstone: phenomena and mechanisms. Eng Geol 276:105760

Chen C-C, Li H-H, Chiu Y-C, Tsai Y-K (2020) Dynamic response of a physical anti-dip rock slope model revealed by shaking table tests. Eng Geol 277:105772

Chen R, Xia K, Dai F, Lu F, Luo SN (2009) Determination of dynamic fracture parameters using a semi-circular bend technique in split Hopkinson pressure bar testing. Eng Fract Mech 76:1268–1276

Doan M-L, d'Hour V (2012) Effect of initial damage on rock pulverization along faults. J Struct Geol 45:113–124

Doan M-L, Gary G (2009) Rock pulverization at high strain rate near the San Andreas fault. Nat Geosci 2:709–712

Dresen G, Guéguen Y (2004) Damage and rock physical properties. Int Geophys Ser 89:169–218

Eberhardt E, Stead D, Stimpson B (1999) Quantifying progressive pre-peak brittle fracture damage in rock during uniaxial compression. Int J Rock Mech Min Sci 36:361–380

Faulkner DR, Mitchell TM, Healy D, Heap MJ (2006) Slip on'weak'faults by the rotation of regional stress in the fracture damage zone. Nature 444:922–925

Field JE, Walley SM, Proud WG, Goldrein HT, Siviour CR (2004) Review of experimental techniques for high rate deformation and shock studies. Int J Impact Eng 30:725–775

Frew DJ, Forrestal MJ, Chen W (2001) A split Hopkinson pressure bar technique to determine compressive stress-strain data for rock materials. Exp Mech 41:40–46

Grady DE (2008) Fragment size distributions from the dynamic fragmentation of brittle solids. Int J Impact Eng 35:1557–1562

Grady DE, Kipp ME (1979) The micromechanics of impact fracture of rock. In: International Journal of Rock Mechanics and Mining Sciences & Geomechanics Abstracts. Elsevier, pp 293–302

Grady DE, Winfree NA (2001) Impact fragmentation of high-velocity compact projectiles on thin plates: a physical and statistical characterization of fragment debris. Int J Impact Eng 26:249–262

Griffith WA, Mitchell TM, Renner J, Di Toro G (2012) Coseismic damage and softening of fault rocks at seismogenic depths. Earth Planet Sci Lett 353:219–230

Griffiths L, Heap MJ, Baud P, Schmittbuhl J (2017) Quantification of microcrack characteristics and implications for stiffness and strength of granite. Int J Rock Mech Min Sci 100:138–150

Huang S, Xia K (2015) Effect of heat-treatment on the dynamic compressive strength of Longyou sandstone. Eng Geol 191:1–7

Huang Y, Ampuero J, Helmberger DV (2014) Earthquake ruptures modulated by waves in damaged fault zones. J Geophys Res Solid Earth 119:3133–3154

Hudson JA, Bäckström A, Rutqvist J, Jing L, Backers T, Chijimatsu M, Christiansson R, Feng X-T, Kobayashi A, Koyama T (2009) Characterising and modelling the excavation damaged zone in crystalline rock in the context of radioactive waste disposal. Environ Geol 57:1275–1297

Kipp ME, Grady DE, Chen EP (1980) Strain-rate dependent fracture initiation. Int J Fract 16:471–478

Li D, Han Z, Sun X, Zhou T, Li X (2019) Dynamic mechanical properties and fracturing behavior of marble specimens containing single and double flaws in SHPB tests. Rock Mech Rock Eng 52:1623–1643

Li SH, Zhu WC, Niu LL, Dai F (2017) Constant strain rate uniaxial compression of green sandstone during SHPB tests driven by Pendulum Hammer. Shock Vib 2017

Li SH, Zhu WC, Niu LL, Yu M, Chen CF (2018a) Dynamic characteristics of green sandstone subjected to repetitive impact loading: phenomena and mechanisms. Rock Mech Rock Eng 51:1921–1936

Li X, Ma C, Qi C, Shao Z (2020a) Crack velocity-and strain rate-dependent dynamic compressive responses in brittle solids. Theor Appl Fract Mech 105:102420

Li X, Main I, Jupe A (2018b) Induced seismicity at the UK 'hot dry rock'test site for geothermal energy production. Geophys J Int 214:331–344

Li X, Zhou Z, Lok T-S, Hong L, Yin T (2008) Innovative testing technique of rock subjected to coupled static and dynamic loads. Int J Rock Mech Min Sci 45:739–748

Li XB, Lok TS, Zhao J (2005) Dynamic characteristics of granite subjected to intermediate loading rate. Rock Mech Rock Eng 38:21–39

Li Y, Zhai Y, Wang C, Meng F, Lu M (2020b) Mechanical properties of Beishan granite under complex dynamic loads after thermal treatment. Eng Geol 267:105481

Ma L, Wu J, Wang M, Dong L, Wei H (2020) Dynamic compressive properties of dry and saturated coral rocks at high strain rates. Eng Geol 272:105615

Martino JB, Chandler NA (2004) Excavation-induced damage studies at the underground research laboratory. Int J Rock Mech Min Sci 41:1413–1426

Mitchell TM, Ben-Zion Y, Shimamoto T (2011) Pulverized fault rocks and damage asymmetry along the Arima-Takatsuki Tectonic Line. Jpn Earth Planet Sci Lett 308:284–297

Moosavi S, Scholtès L, Giot R (2018) Influence of stress induced microcracks on the tensile fracture behavior of rocks. Comput Geotech 104:81–95

Peng J, Rong G, Cai M, Yao M-D, Zhou C-B (2016) Physical and mechanical behaviors of a thermal-damaged coarse marble under uniaxial compression. Eng Geol 200:88–93

Roy MP, Singh PK (2016) Blast design and vibration control at an underground metal mine for the safety of surface structures. Int J Rock Mech Min Sci 83:107–115

Souley M, Homand F, Pepa S, Hoxha D (2001) Damage-induced permeability changes in granite: a case example at the URL in Canada. Int J Rock Mech Min Sci 38:297–310

Walsh JB (1965) The effect of cracks on the compressibility of rock. J Geophys Res 70:381–389

Wang P, Xu J, Fang X, Wang P (2017) Energy dissipation and damage evolution analyses for the dynamic compression failure process of red-sandstone after freeze-thaw cycles. Eng Geol 221:104–113

Wu Z, Liang X, Liu Q (2015) Numerical investigation of rock heterogeneity effect on rock dynamic strength and failure process using cohesive fracture model. Eng Geol 197:198–210

Xia K, Nasseri MHB, Mohanty B, Lu F, Chen R, Luo SN (2008) Effects of microstructures on dynamic compression of Barre granite. Int J Rock Mech Min Sci 45:879–887

Xia K, Yao W (2015) Dynamic rock tests using split Hopkinson (Kolsky) bar system–a review. J Rock Mech Geotech Eng 7:27–59

Xie H, Gao F, Zhou H, Zuo J (2003) Fractal fracture and fragmentation in rocks. J Seismol

Yan C (2007) Blasting cumulative damage effects of underground engineering rock mass based on sonic wave measurement. J Cent South Univ Technol 14:230–235

Yu L, Fu A, Yin Q, Jing H, Zhang T, Qin H (2020) Dynamic fracturing properties of marble after being subjected to multiple impact loadings. Eng Fract Mech 106988

Yuan F, Prakash V, Tullis T (2011) Origin of pulverized rocks during earthquake fault rupture. J Geophys Res Solid Earth 116

Zhang QB, Zhao J (2014a) A review of dynamic experimental techniques and mechanical behaviour of rock materials. Rock Mech Rock Eng 47:1411–1478

Zhang QB, Zhao J (2014b) Quasi-static and dynamic fracture behaviour of rock materials: phenomena and mechanisms. Int J Fract 189:1–32

Zhou T, Dong SL, Zhao GF, Zhang R, Wu SY, Zhu JB (2018) An experimental study of fatigue behavior of granite under low-cycle repetitive compressive impacts. Rock Mech Rock Eng 51:3157–3166

Zhou YX, Xia K, Li XB, Li HB, Ma GW, Zhao J, Zhou ZL, Dai F (2011) Suggested methods for determining the dynamic strength parameters and mode-I fracture toughness of rock materials. In: The ISRM Suggested Methods for Rock Characterization, Testing and Monitoring: 2007–2014. Springer, pp 35–44

Zhou Z, Li X, Ye Z, Liu K (2010) Obtaining constitutive relationship for rate-dependent rock in SHPB tests. Rock Mech Rock Eng 43:697–706

Zhu WC, Bai Y, Li XB, Niu LL (2012) Numerical simulation on rock failure under combined static and dynamic loading during SHPB tests. Int J Impact Eng 49:142–157

Zuo QH, Addessio FL, Dienes JK, Lewis MW (2006) A rate-dependent damage model for brittle materials based on the dominant crack. Int J Solids Struct 43:3350–3380